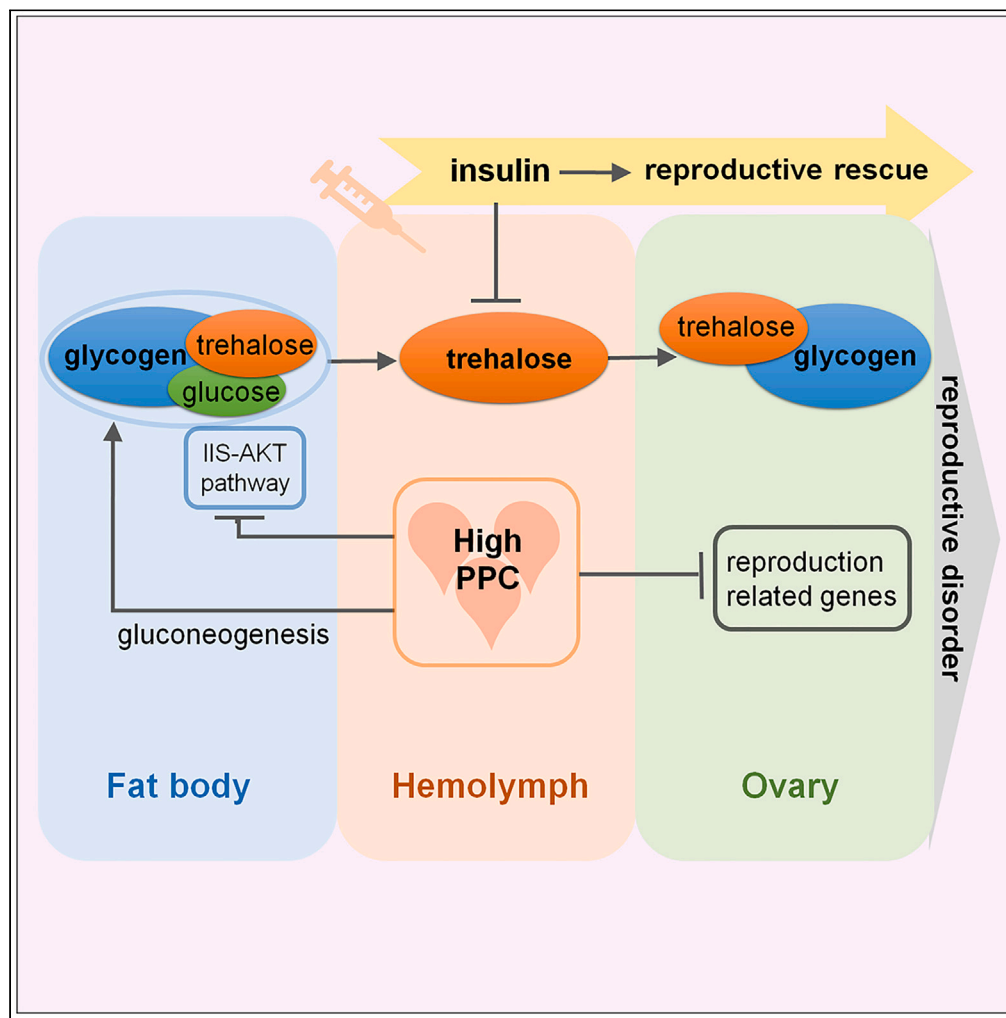


Article

# Mechanism of hyperproteinemia-induced damage to female reproduction in a genetic silkworm model



Gui-Hua Jiang,  
Guang Wang,  
Cheng Luo, ..., Ru-  
Ji Peng, Yang-Hu  
Sima, Shi-Qing Xu

szsqxu@suda.edu.cn

Highlights

A heritable silkworm model of hyperproteinemia with impaired reproduction is reported

High PPC disturbs ovarian sugar metabolism by inducing hyperglycemia

Insulin can effectively reduce female reproductive damage caused by high PPC

Jiang et al., iScience 26, 107860  
October 20, 2023 © 2023 The  
Author(s).  
[https://doi.org/10.1016/  
j.isci.2023.107860](https://doi.org/10.1016/j.isci.2023.107860)



## Article

## Mechanism of hyperproteinemia-induced damage to female reproduction in a genetic silkworm model

Gui-Hua Jiang,<sup>1,2,3</sup> Guang Wang,<sup>1,2,3</sup> Cheng Luo,<sup>1,2</sup> Yong-Feng Wang,<sup>1,2</sup> Jian-Feng Qiu,<sup>1,2</sup> Ru-Ji Peng,<sup>1,2</sup> Yang-Hu Sima,<sup>1,2</sup> and Shi-Qing Xu<sup>1,2,4,\*</sup>

## SUMMARY

**Hyperproteinemia is a metabolic disorder characterized by abnormally elevated plasma protein concentrations (PPC) in humans and animals. Here, a genetic silkworm model with high PPC was employed to investigate the effect of elevated PPC on female reproduction. Transcriptomic analysis revealed that high PPC induces downregulation of the ovarian development-related genes and disrupts ovarian sugar metabolism. Biochemical and endocrinal analyses revealed that high PPC increases trehalose and glucose levels in hemolymph and glycogen content in the fat body through activation of the gluconeogenic pathway and inhibition of the Insulin/Insulin-like growth factor signaling pathway-the serine/threonine kinase (IIS-AKT) pathway, thus disrupting characteristic metabolic homeostasis of sugar in the ovary. These resulted in ovarian developmental delay as well as reduced number and poor quality of eggs. Insulin supplementation effectively increased egg numbers by lowering blood sugar. These collective results provide new insights into the mechanisms by which high PPC negatively affects female reproduction and support the potential therapeutic effects of insulin.**

## INTRODUCTION

Hyperproteinemia is a metabolic disease characterized by abnormally elevated plasma protein concentrations (PPC). Since the first clinical case was initially reported more than 90 years ago, hyperproteinemia has been diagnosed in humans and 11 animal species as a complication of more than 50 major diseases and severe infections, most commonly, kidney disease,<sup>1</sup> liver disease,<sup>2</sup> multiple myeloma,<sup>3,4</sup> visceral leishmaniasis and plasmacytoma.<sup>5-7</sup>

To date, no cases of hyperproteinemia without primary disease have been identified. The concurrent relationship between the two is unknown, making it difficult to distinguish the biological effects of hyperproteinemia from those of primary disease or infection.<sup>8</sup> Manning created a canine hyperproteinemia model by intravenously infusing autologous plasma to investigate the effects of increasing PPC on renal hemodynamics, fluid volume, and arterial pressure.<sup>9</sup> However, the canine model is not acceptable for clinical application due to poor repeatability, difficulty in preparation, high cost, and ethical issues. According to previous reports, plasma samples from patients and animals with hyperproteinemia showed significant increases in various endogenous proteins, such as globulin, fibrinogen, and albumin.<sup>3,10,11</sup> These data indicate that the damage mechanism underlying hyperproteinemia may be related to the metabolic imbalances in the circulatory system rather than the increase of a single protein. Owing to the lack of suitable animal models, the analysis of the underlying pathological mechanisms and the development of related therapeutic drugs are severely restricted, highlighting the urgent clinical requirement for animal models of high PPC without primary disease.

An abundance of research has demonstrated that metabolic abnormalities in the circulatory system can exert significant adverse effects and complex mechanisms on the reproductive development of humans and other animals.<sup>12-16</sup> For instance, Wistar Audiogenic Rats with hyperproteinemia produced embryos and fetuses with poor viability and newborns with impaired development.<sup>17</sup> Additionally, hyperproteinemia is also known to significantly reduce the number of transferable embryos in donor cows.<sup>18</sup> However, the mechanisms by which hyperproteinemia affects female reproduction are still unclear. Therefore, it is necessary to develop a high PPC model without the impact of primary diseases and use it to evaluate the damage and mechanisms associated with high PPC on reproduction.

Silkworm (*Bombyx mori*) is currently a dominant animal model for studying the impact mechanism of high PPC.<sup>8,19,20</sup> One of the remarkable physiological characteristics of silkworm is that its larval silk gland can efficiently synthesize and store non-toxic silk protein that accounts for 20–35% of its body weight.<sup>21,22</sup> After the larvae mature, most silk proteins are secreted outside the body. In the late stages of silk secretion, the silk gland begins to undergo programmed degeneration until disappearance and silk protein remaining in the silk gland cavity is subsequently released into the hemolymph, causing a transient increase in PPC.<sup>8,19,20</sup> This indicates that the silkworm has a strong ability to regulate PPC elevation. Based on this physiological feature, a primary animal model of hyperproteinemia (AM) with a 6- to 8-fold increase in PPC was

<sup>1</sup>School of Biology and Basic Medical Sciences, Suzhou Medical College, Soochow University, Suzhou 215123, China

<sup>2</sup>Institute of Agricultural Biotechnology & Ecology (IABE), Soochow University, Suzhou 215123, China

<sup>3</sup>These authors contributed equally

<sup>4</sup>Lead contact

\*Correspondence: szsqxu@suda.edu.cn

<https://doi.org/10.1016/j.isci.2023.107860>



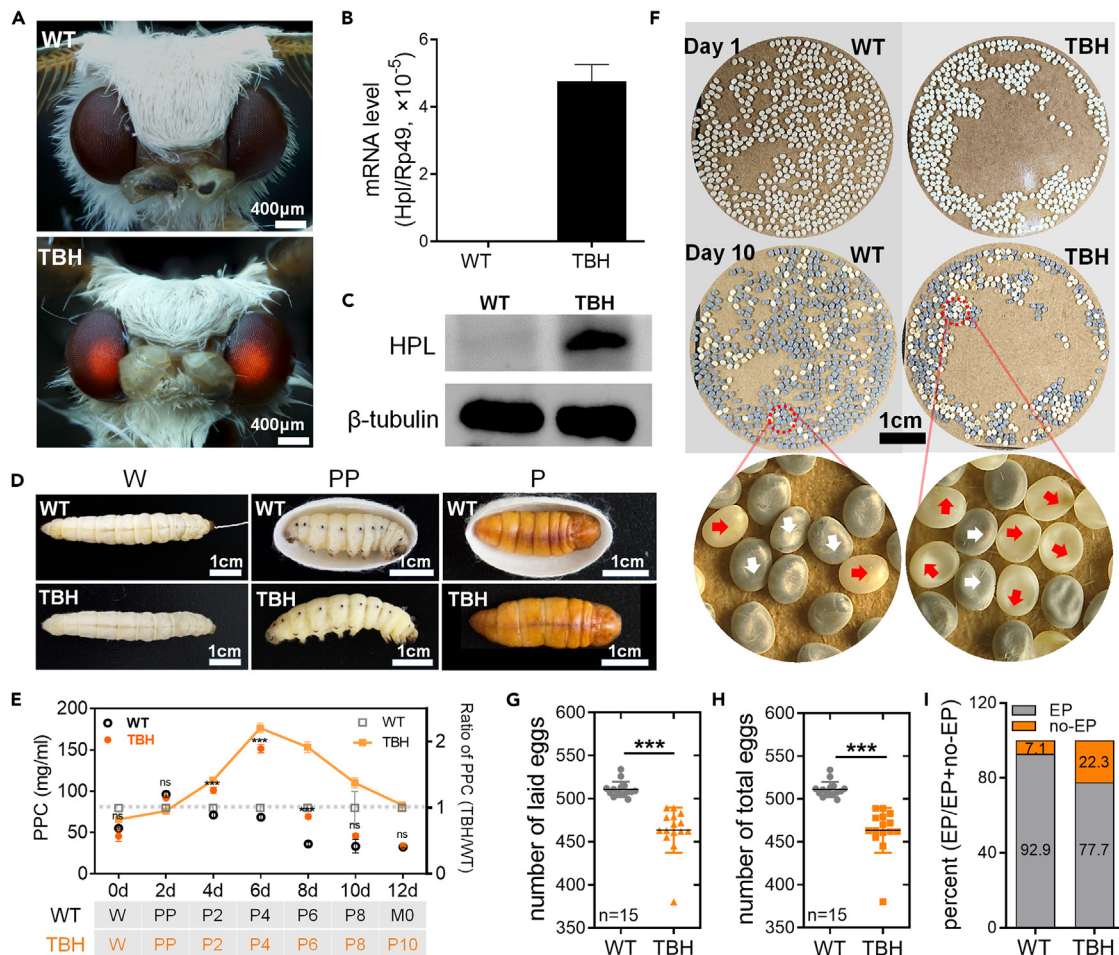


**Figure 1. Impact of high PPC on the number and quality of silkworm eggs**

(A) Compound eyes of adults. The compound eyes showed red fluorescence due to the ERFP (Ds-Red) reporter gene in the transgenic mutant TBH.

(B) Transcription level of *Hpl* gene in the silk gland was detected by qRT-PCR. *Rp49* was used as the internal reference gene.  $n = 3$ .

(C) Levels of HPL protein in the silk gland were analyzed by Western blotting. HPL protein is 68 kD, and the reference  $\beta$ -tubulin protein is 55 kD.

(D) Metamorphosis of TBH and WT. W, wandering stage, mature larvae begin to spin silk and form cocoons. PP, prepupal stage, the end of spinning and cocooning. P, pupal stage, complete larval-pupal metamorphosis development.

(E) PPC. P2-P10, pupa age 2 days–10 days. M0, newly molted adult stage.  $n = 3$ .

(F) Morphology of eggs. Day 1, just laid eggs; Day 10, eggs in the body pigmentation stage (EP), near hatching. The white arrow shows the eggs in EP and the red arrow shows eggs in the body no-pigmentation stage (no-EP).

(G) Number of laid eggs ( $n = 15$ ).

(H) Total number of eggs ( $n = 15$ ).

(I) EP rate ( $n = 6$ ).

The data were mean  $\pm$  SD, and the significance of the difference in the Student's *t* test was ns,  $p > 0.05$ ; \*,  $p < 0.05$ ; \*\*,  $p < 0.01$ ; \*\*\*,  $p < 0.001$ .

constructed by blocking the silk hole of the mature larvae to prevent the silk protein from being secreted out.<sup>19,20</sup> This endogenous non-toxic silk protein dose not induce immune rejection but effectively simulates clinical hyperproteinemia. In addition, compared with the canine hyperproteinemia model,<sup>9</sup> the advantages of high PPC silkworm model include exceptional repeatability and stability, affordability, easy accessibility, and the absence of ethical concerns. Here, we explored the molecular targets of high PPC in the female reproductive system via ovarian transcriptome sequencing and further uncovered the underlying mechanisms of disruption of the energy metabolism using a genetic silkworm model of high PPC.

## RESULTS

### High PPC hinders ovarian development and affects the quantity and quality of offspring

TBH silkworm is a stable transgenic strain. As shown in Figure 1A, the compound eyes of TBH adults displayed red fluorescence produced by the reporter gene, which was absent in its WT counterpart. Data from qRT-PCR and Western blot showed normal transcription and translation

of exogenous *Hpl* in the larval silk glands (Figures 1B and 1C). TBH could complete the metamorphosis process similar to WT and the morphological characteristics of larvae, pupae, and adults were normal (Figure 1D). The major differences were that TBH silkworm could not spin silk to form cocoons, in contrast to mature WT larvae (W stage), and the development speed of pupae was slower at the later stage (Figures 1D and 1E).

As shown in Figure 1E, the PPC of WT increased transiently by nearly 1-fold, accompanied by degradation of silk glands and release of silk proteins into hemolymph in the prepupal stage (PP), but PPC returned to normal levels within 48 h. These findings suggest that silkworm has acquired physiological adaptability to PPC changes over its evolutionary history. Interestingly, although PPC of TBH silkworm was extremely similar to that of WT from the third day of the fifth-instar larval (L5D3) to the PP stage, the levels continued to increase until P4 stage to a peak concentration over 3 times higher than that at the W stage and 2.5 times higher than WT at the equivalent time-points (Figures 1E and S1A). A ~100 h time window of high PPC (from P2 to P6) was detected in TBH silkworm (Figure 1E).

Almost all organs, such as the gonads, are suspended in the open circulatory system. Our results showed that high PPC is the specific phenotype of TBH in the early and middle stages of pupal growth, and the time window in which high PPC occurs is a critical period of female reproductive development that is similar to human adolescence. The duration during which the ovaries were exposed to the high PPC environment accounted for 40% of the whole pupal stage (Figure 1E). Accordingly, we explored the effect of high PPC on female reproduction using TBH as the model silkworm. Our data showed that the number of eggs produced and laid by TBH adults was significantly lower than that by WT (Figures 1F–1H). Importantly, the rate of eggs in the body pigmentation stage (EP), representing a comprehensive index of egg quality, was significantly lower, and the rate of eggs in the body no-pigmentation stage (no-EP) was up to 22.3%, nearly three times higher than that of WT (7.1%) (Figures 1F, 1I, and S1B). Furthermore, most eggs from the no-EP group were unfertilized, resulting in desiccation and loss of moisture due to the absence of serosal protection (Figure 1F). The collective findings indicate that high PPC seriously affects the quantity and quality of offspring.

The left and right ovaries of silkworm are composed of four ovarian tubes, which converge to form oviducts at the end of the tubes in the late pupal stage. The average length of the eight ovarian tubes of the model silkworm was 17% shorter and the weight of intact ovaries was 13% lower than that of WT (Figures 2A, 2B, and S2), indicating that the decrease in egg number of the model silkworm with high PPC is associated with a delay in ovarian development. To determine the period of ovarian development sensitive to the effects of high PPC, morphological characteristics before and after elevation of PPC were monitored. The results showed that at the W stage before the increase in PPC, ovarian morphology and size were similar between the model silkworm and WT, developmental progress in tissue was analogous, and both had complete ovarian outer membranes (Figure 2C). At the PP stage accompanying the physiological increase in PPC, the ovarian outer membrane of the model silkworm did not rupture with development in contrast to WT, clearly indicating a developmental lag in the ovaries of the model silkworm (Figure 2D).

The difference in ovarian development between the model silkworm and WT during the high PPC window was more significant (Figure 2E). Silkworm eggs enter choriogenesis in the middle pupal stage, during which the eggs almost mature and become white in color due to excess water absorption. During the P6 stage, the ovarian tubes of the model silkworm exhibited the initial emergence of mature eggs, whereas in the WT group, the count had already reached approximately 50% of that observed in the adult stage (Figures 2F and 2G). Systematic analysis of the weights of ovaries and gonadosomatic index before and after the increase in PPC further confirmed greater developmental differences in the ovary during the high PPC window between the model silkworm and WT groups (Figures 2H and 2I).

Notably, the difference in the number of mature eggs between the model silkworm and WT during the P6 stage was significantly larger than that in the adult stage (Figures 1H and 2G). Moreover, the difference in ovarian weight during the high PPC window (P4–P6) was more pronounced between the two groups (Figures 2B and 2H). Our results suggest that the model silkworm tends to compensate for the developmental lag to a certain extent by prolonging the ovarian development process after PPC returns to normal physiological levels, but fails to fully recover to the WT level.

### High PPC downregulates development-related genes and disrupts sugar metabolism in the ovary

To identify the molecular targets of high PPC that affect female reproduction, RNA-seq analysis was performed on ovarian tissues at the P2 and P4 stages (Figure 3A). Principal component analysis (PCA) and heatmap data showed good reproducibility among samples within groups and significant differences between groups, indicating reliable sequencing results (Figures 3B and S3). In the analysis of differentially expressed genes (DEGs) with WT as the control (Figure 3C), the number of DEGs of the model silkworm at P4 was 1.9 times higher than that at P2 and the number of downregulated genes exceeded the number of upregulated genes by 50%, corresponding to the greater difference in developmental progress between WT and model silkworm with elevated PPC. This phenomenon was further validated by the finding that the number of DEGs (T4 vs. T2) of the model silkworm was much lower than the corresponding stages of WT (W4 vs. W2). The number of downregulated genes was similar (288/291), while the number of upregulated genes in the model silkworm group was only 55% (260/471) of that in WT group.

Focusing on the DEGs related to ovarian development, six genes were significantly downregulated at the P2 and P4 stages of the model silkworm group, including estrogen-related receptor gene (*ESRRA*), zinc transporter gene (*ZIP3*), a developmental regulator of offspring embryos, carbonic anhydrase gene (*CA7*) that stabilizes extracellular pH, and three genes involved in oocyte maturation, including mitochondrial S-adenosylmethionine (SAM) transporter gene (*SLC25A26*), 5-hydroxytryptamine receptor gene (*5-HTR*), and  $\gamma$ -GABA receptor gene (*GABBR*) (Figure 3D). These results suggest that the downregulation of these genes induced by high PPC is related to significantly slower ovarian development.

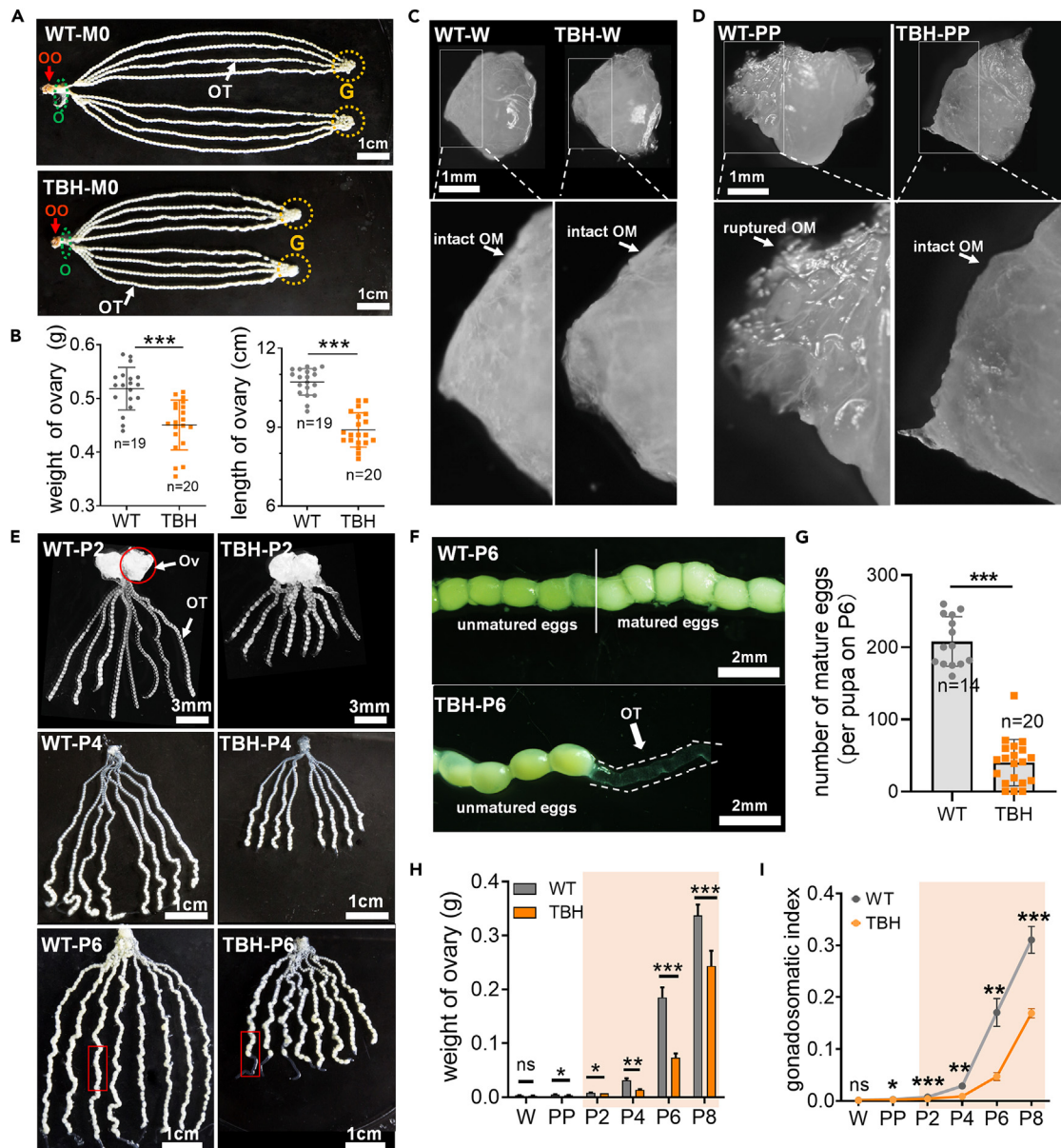


**Figure 2. Impact of high PPC on the ovarian development**

(A) Adult ovary. M0, newly molted adult stage. G, germarium. OO, oviporous orifice. O, oviductus. OT, ovarian tube.

(B) Weight and length of ovaries in M0.

(C) Ovaries with similar morphology in W. OM, ovarian outer membrane.

(D) Ovaries with different morphology in PP. Ruptured OM indicates faster ovarian development.

(E) Developmental morphology of ovaries in P2-P6.

(F) Development status of eggs in P6. Enlarged view of the ovarian tube with the red box in (E). Mature eggs appear white.

(G-I) Number of mature eggs in P6. Ovarian weight (H) and Gonadosomatic index (I) from W to P8 stages (n = 3).

Data in (B, G, H, and I) were the mean  $\pm$  SD, and the significance of the difference in the Student's t test was ns,  $p > 0.05$ ; \*,  $p < 0.05$ ; \*\*,  $p < 0.01$ ; \*\*\*,  $p < 0.001$ .

The reproductive development of silkworm, like other ovipara, requires a large amount of carbohydrates, mainly in the form of trehalose, which is absorbed from the hemolymph and stored as glycogen in the ovary. Interestingly, *Tret1*, which encodes a trehalose-specific transporter, ranked fifth in the list of upregulated DEGs of the model silkworm at both the P2 and P4 stages (Figure 3E). qRT-PCR results confirmed that *Tret1* is markedly upregulated in the ovary of the model silkworm, suggesting abnormal trehalose absorption (Figure 3E'). Additionally, the trehalose content in ovary of the model silkworm at the selected P4 stage was significantly higher compared to WT and the mRNA level of the *trehalase2* gene in ovary during the high PPC window was significantly up-regulated (Figures 3F and 3G). Further investigation revealed a

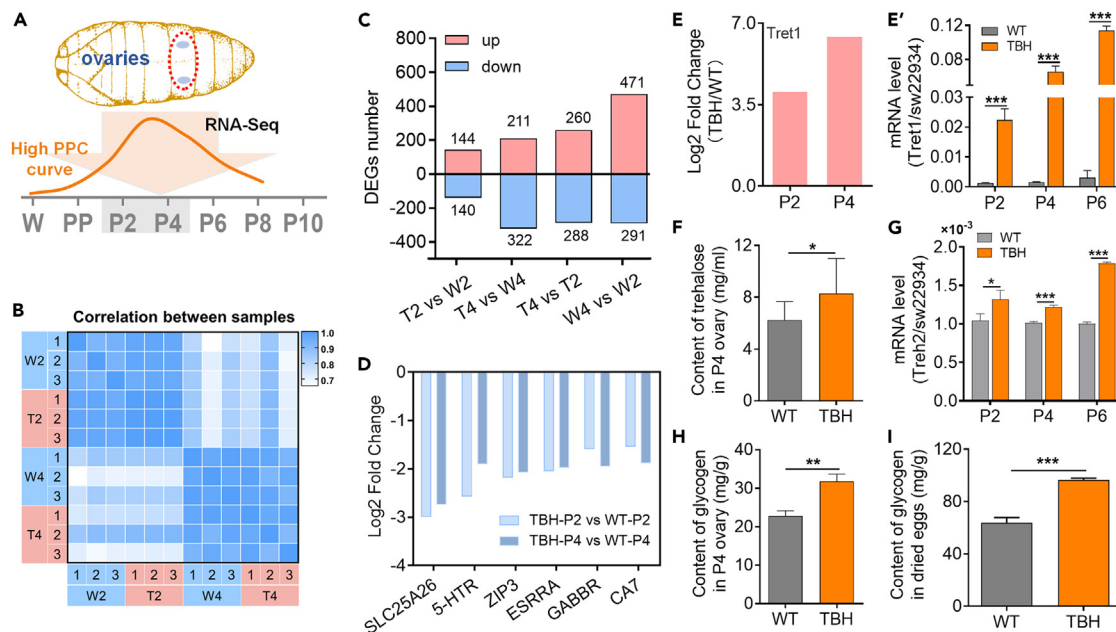


**Figure 3. High PPC downregulates development-related genes and disrupts sugar metabolism in the ovary**

(A) RNA-seq timeline. The ovaries in P2 and P4 with the significantly increasing PPC were used for RNA-seq.

(B) Heatmap of sample correlation analysis. T2 and T4 represent TBH in P2 and P4, respectively. W2 and W4 represent WT in P2 and P4, respectively.

(C) Number of DEGs.

(D) Relative expression of genes related to ovarian development (TPM). *SLC25A26*, mitochondrial SAM transporter gene; *5-HTR*, 5-hydroxytryptamine receptor gene; *ZIP3*, zinc transporter ZIP3 gene; *ESRRA*, estrogen related receptor gene; *GABBR*,  $\gamma$ -GABA receptor gene; *CA7*, carbonic anhydrase 7. The vertical axis shows the ratio of expression changes of different genes with WT as control (log<sub>2</sub> Fold change).

(E and E') Relative expression of *Tret1* (TPM) and qRT-PCR validation results (n = 3). *Tret1*, facilitated trehalose transporter1.

(F) Trehalose content in the P4 ovary (n = 3).

(G) Relative expression of *Treh2* (n = 3). *Treh2*, trehalase2 gene.

(H and I) Glycogen content in the P4 ovary (H) and laid egg (I) (n = 3). *sw22934* was used as the reference gene for qRT-PCR.

The data of (E'–I) were mean  $\pm$  SD, and the significance of the difference in the Student's t test was \*, p < 0.05; \*\*, p < 0.01; \*\*\*, p < 0.001.

significant increase in glycogen accumulation in the P4 ovary and laid eggs of the TBH model compared to the WT silkworm (Figures 3H and 3I). These findings suggest that high PPC induces abnormal trehalose absorption in the ovary, further leading to excessive accumulation of glycogen, which affects egg quality.

### High PPC induces hyperglycemia by activating the gluconeogenesis pathway

The blood sugar of silkworm mainly consists of trehalose, along with a small amount of glucose. The contents of trehalose and glucose in hemolymph of the pupal stage were significantly increased in the model silkworm (Figure 4A). Glucose level were similar to those of the control group at the end of the high PPC window, whereas the trehalose content was further increased (Figure 4A).

The fat body, similar to the mammalian liver, regulates blood sugar in silkworm. The fat body mass coefficient of the model silkworm at the P6 stage was significantly higher than that of WT, along with a higher glycogen content stored in the fat body (Figures 4B and S4A). A high PPC model (mAM) was reconstructed to further validate the hyperglycemia observed in the TBH model. These results confirmed hyperglycemia in mAM in which the PPC level was close to that of the TBH model (Figure S4B). There were no significant differences in the contents of trehalose and glucose in hemolymph and glycogen in the fat body when comparing TBH and WT silkworms at the L5D3 and W stage (Figure S4C). These results suggest that high PPC induces hyperglycemia.

The main amino acid residues (90%) of silk protein in silkworm are tyrosine, alanine, glycine, and serine. Considering that excessive amino acids hydrolyzed from proteins in the circulating blood of silkworm can be converted into carbohydrates in the fat body through the gluconeogenesis pathway, we investigated the contents of these four amino acids and the transcription levels of the genes encoding related metabolic enzymes. The levels of the aforementioned four amino acids in hemolymph were significantly increased (Figure S4D), and the amino acid transporter gene in the fat body was also significantly up-regulated in the model silkworm group (Figure S4E). Furthermore, transcription levels of key genes of the gluconeogenesis pathway involved in the conversion of these four amino acids in the fat body were significantly upregulated to different degrees, while only *SHMT* was significantly downregulated in the P6 phase (Figure 4C). mRNA levels of the key genes of trehalose and glycogen synthesis were also markedly elevated (Figures 4D and 4E). Based on these findings, we propose that hyperglycemia induced by high PPC is associated with the activation of the gluconeogenesis pathway.

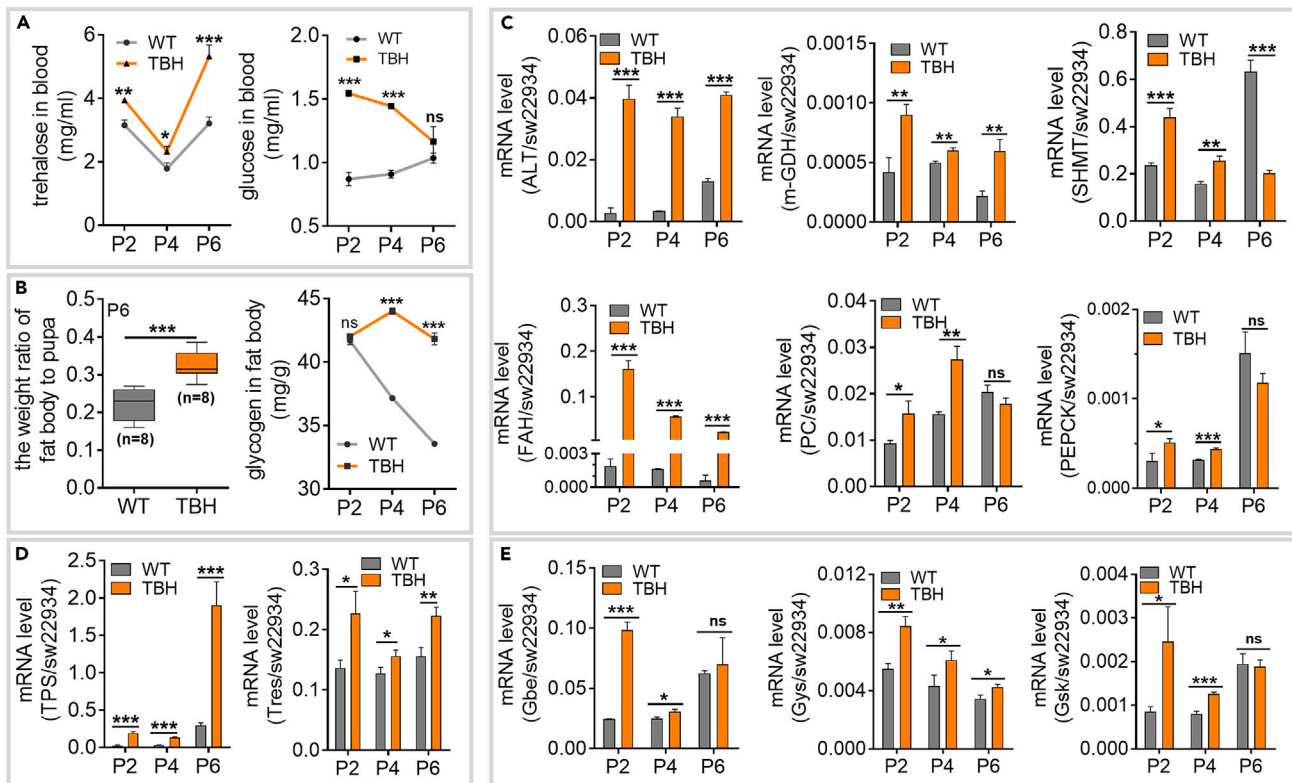


**Figure 4. High PPC induces hyperglycemia by activating the gluconeogenic pathway**

(A) Trehalose and glucose levels in hemolymph (n = 3).

(B) Fat body index and glycogen content in the fat body (n = 3). Fat body index = fat body weight/pupa weight.

(C) Transcription levels of key genes of the gluconeogenesis pathway involved in the conversion of alanine, glycine, tyrosine, and serine were determined by qRT-PCR (n = 3). *ALT*, alanine aminotransferase gene; *m-GDH*, glutamate dehydrogenase gene; *SHMT*, serine hydroxymethyl transferase gene; *FAH*, fumarase gene; *PC*, pyruvate carboxylase gene; *PEPCK*, phosphoenolpyruvate carboxykinase gene.

(D) Relative expression of genes related to trehalose synthesis (n = 3). *TPS*, trehalose-6-phosphate synthase gene; *Tres*, trehalose synthetase gene.

(E) Transcriptional level of key genes for glycogen synthesis (n = 3). *Gbe*, glycogen branching enzyme gene; *Gys*, glycogen synthase gene; *Gsk*, glycogen synthase kinase gene. *sw22934* was used as the reference gene for qRT-PCR.

The data were mean  $\pm$  SD, and the significance of the difference in the Student's t test was ns,  $p > 0.05$ ; \*,  $p < 0.05$ ; \*\*,  $p < 0.01$ ; \*\*\*,  $p < 0.001$ .

### Insulin supplementation can effectively reduce female reproductive damage caused by high PPC

To verify whether hyperglycemia impairs female reproduction, trehalose was injected into the body fluids of WT to simulate the hyperglycemic conditions of TBH. Hyperglycemia caused by trehalose injection continued to the P6 stage (Figure 5A), and further induced a significant reduction in the number of eggs produced and laid by adult silkworms (Figure 5A'). These results support the detrimental effect of abnormally elevated trehalose levels in hemolymph on female reproduction.

Further investigation of the classical pathway of blood sugar regulation revealed that the phosphorylated AKT level in the model silkworm was decreased, consistent with the phenomenon of hyperglycemia (Figure 5B). After injection of the insulin signaling pathway inhibitor LY294002 into WT, the number of eggs made and laid by females was significantly reduced, similar to the reproductive characteristics of the model silkworm (Figure 5C). After supplementation with bovine insulin in the model silkworm to determine the effective dose range, we observed that injection of 100  $\mu$ g bovine insulin per pupa led to a decrease in trehalose and glucose levels in hemolymph and a significant increase in the number of eggs made and laid by adults (Figures 5D, 5D', 5S5A, and 5S5B). It is worth noting that there was no significant difference in the number of eggs produced and laid by the model silkworm after insulin injection when compared to the WT group. Upon injection of the same dose of insulin into WT, blood sugar was lower than that of the control group, and the number of eggs produced and laid by adults was significantly reduced (Figures 5E and 5E'). The combined findings suggest that the addition of insulin effectively mitigates the adverse impact of high PPC on female reproduction by lowering blood sugar.

## DISCUSSION

The silkworm has been utilized as a model animal by the International Society of Invertebrate Pathology (SIP) since 2002. Due to its abundant mutants, clear genetic background, moderate individual size, ease of operation, short generation cycle, simple feeding requirements, and

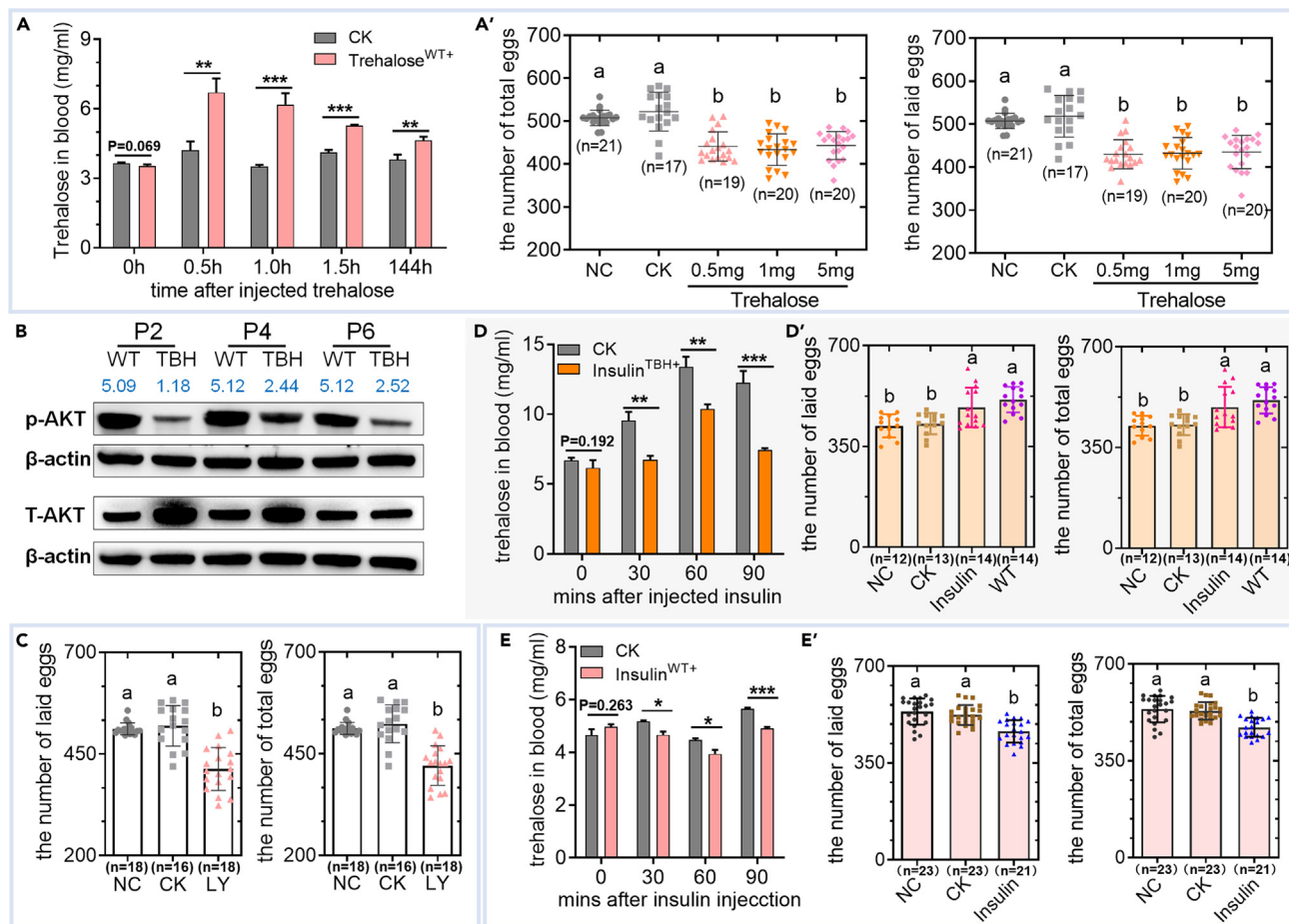


**Figure 5. Effects of insulin on the reproduction of model silkworm by regulating blood sugar**

(A) Trehalose level in hemolymph (n = 3).

(A') Egg number after trehalose injection in WT. Trehalose (0.5, 1.0, or 5.0 mg per pupa) was injected into WT in the P1 stage, and the number of eggs produced and laid was counted at the adult stage. Hemolymph samples were collected at 0, 0.5, 1.0, 1.5, and 144 h after 1.0 mg trehalose injection per pupa.

(B) Total AKT and phosphorylated AKT protein levels in the fat body. The gray values were calculated using ImageJ and the blue data represent the gray value ratio of P-AKT/ $\beta$ -actin and AKT/ $\beta$ -actin. The protein of AKT and P-AKT is 60 kD, and the protein of  $\beta$ -actin is 42 kD.

(C) Egg number of WT injected with LY294002. LY294002 (LY), a PI3K/Akt signaling pathway inhibitor, was injected into body fluids at a dose of 0.001 nmol per pupa in P1, and the number of eggs produced and laid was counted at the adult stage.

(D and E) Trehalose level in hemolymph (D and E) and Egg number (D' and E') after bovine insulin supplementation respectively in TBH and WT silkworm. Bovine insulin was injected into the body fluid in P1 at a dose of 100  $\mu$ g per pupa. The hemolymph samples (n = 3) were collected at 0, 30, 60, and 90 min after injection to investigate the trehalose content and further count the number of eggs made and laid at the adult stage. The control (CK) was injected with the same volume of saline solution.

NC, negative control. Except for (B), the data in the figures were the mean  $\pm$  SD. The data in (A, D, and E) were analyzed by the Student's t test and the significance of the difference was \*, p < 0.05; \*\*, p < 0.01; \*\*\*, p < 0.001. The data in (A', C, D', and E') were analyzed by ANOVA, and the different letter among groups presents a significant difference.

low cost, this model is employed to study various metabolic diseases, such as hyperuricemia, sepiapterin reductase deficiency, and diabetes.<sup>26–29</sup>

Data obtained from the AM silkworm model showed that high PPC significantly affected cell regeneration of the fat body and disrupted the function of amino acid transformation by weakening the effects of endocrine hormones and increasing oxidative stress.<sup>19</sup> High PPC induced a marked increase in antimicrobial peptides and antibacterial activity in the hemolymph of AM through the Toll and Imd pathways in NF- $\kappa$ B signaling, but inhibited hemolymph melanization.<sup>20</sup> Additionally, under conditions of high PPC, proliferation of blood cells dominated by granulosa cells was induced via activation of the JAK/STAT signal pathway, along with the occurrence of programmed cell death in blood cells dependent on the calcium ion signal pathway of endoplasmic reticulum, ultimately leading to severe disruption of blood cell homeostasis.<sup>8</sup> Supplementation of 20-hydroxyecdysone (20E), an endocrine regulator of development and reproduction in silkworm, significantly reduced the adverse effects of high PPC on the homeostasis of circulating blood cells, and the regeneration and function of the fat

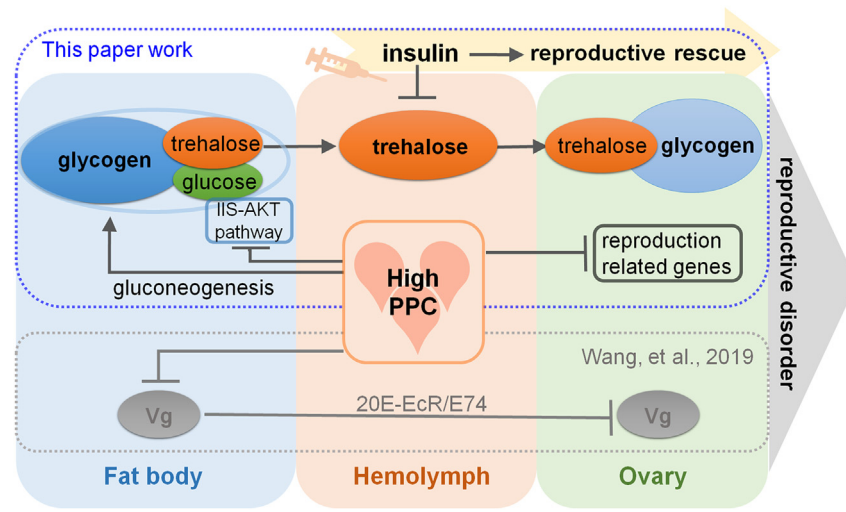


**Figure 6. Summary of the impact of high PPC on female reproduction**

High PPC induces an increase of trehalose level in hemolymph and glycogen content in the fat body by activating the gluconeogenesis pathway and inhibiting the IIS-AKT pathway, subsequently increasing absorption of trehalose and glycogen accumulation in the ovary. Simultaneously, genes related to ovarian development are downregulated, ultimately leading to female reproductive disorders. Insulin effectively rescues reproductive damage by reducing the blood sugar level. Previous studies indicate that high PPC inhibits the synthesis and absorption of Vg, resulting in reproductive damage.<sup>35</sup> The blue dotted line box represents our research results and the gray dotted line box represents the work of Wang et al. The flat heads denote an inhibitory effect, while arrows signify a promotional effect.

body.<sup>8,19</sup> Clearly, elevated PPC has adverse and complex effects on various key organs. Findings from the silkworm model provide experimental animal evidence of the impact of high PPC on health and create preliminary reference guidelines for future research on hyperproteinemia in mammals and humans. Given the complex and critical influence of the blood metabolic environment, the development of animal models that can be explored from further perspectives is essential.

Characteristically, primary oocytes absorb a large quantity of vitellogenin (Vg) and trehalose during ovarian development of female silkworm.<sup>30,31</sup> Vg in silkworm is synthesized in the fat body, secreted into the hemolymph, and ingested into oocytes by endocytosis via the vitellogenin receptor (VgR) on the ovarian membrane.<sup>32</sup> Following the interaction of 20E with ecdysone receptor/ultraspiracle protein (EcR/USP), expression of Vg and VgR genes is regulated by a cascade reaction, which promotes the synthesis and absorption of Vg and accelerates the formation of eggs.<sup>30,33</sup> In addition, estrogen also utilizes EcR as a “receptor” to induce the expression of ESRRA which further participates in the 20E signaling pathway to regulate Vg expression.<sup>34</sup> Experiments using the high PPC model (AM) have showed that the expression of Vg in the fat body and VgR in the ovary is significantly reduced, and the effect of the 20E pathway is weakened, resulting in reduced transport and accumulation of Vg within the ovary.<sup>35</sup> In this study, the downregulation of Vg in the fat body and *ESRRA* in the ovary in genetically high PPC silkworm further supports the theory that high PPC affects female reproduction by inhibiting Vg protein synthesis and absorption, which is regulated by the endocrine hormone (20E) pathway (Figures S5C and 3D).

Clinical studies have shown that disorders in glucose metabolism are seriously harmful to the female reproductive system and offspring of women with diabetes have a higher probability of malformation and death.<sup>36,37</sup> In rodent models, maternal hyperglycemia affects development from the single-cell zygote to blastocyst stage and reduces the glucose utilization rate of mouse embryos before implantation.<sup>38</sup> Abnormalities of characteristic sugar metabolism in silkworm ovaries also affect the development of eggs.<sup>24</sup> In our experiments, high PPC in the genetic silkworm model increased the levels of trehalose and glucose in hemolymph through the activation of the gluconeogenesis pathway and inhibition of the Insulin/Insulin-like growth factor signaling pathway—the serine/threonine kinase (IIS-AKT) pathway. Consequently, trehalose absorption and glycogen accumulation in the ovaries were disrupted. Following injection of insulin, the blood sugar level of the model silkworm decreased and the number of eggs made and laid increased. Additionally, the expression of Vg gene was significantly downregulated in the model silkworm and WT with high trehalose levels, which was reversed with insulin supplementation (Figures S5C–S5E). Based on these findings, we propose that high PPC has detrimental effects on female reproduction by affecting blood sugar levels and Vg synthesis pathways. Therefore, the endocrine active substances, insulin and 20E, may have potential as therapeutic drugs for high PPC.

## Conclusion

In summary (Figure 6), high PPC induces abnormal trehalose absorption in the ovary and excessive accumulation of glycogen in mature eggs by stimulating the gluconeogenesis pathway and inhibiting the IIS-AKT pathway, and downregulates genes related to ovarian development, ultimately resulting in ovarian retardation as well as a reduced number and poor quality of eggs. Insulin supplementation effectively reduces reproductive damage caused by high PPC by lowering blood sugar.

### Limitations of the study

In this article, we utilized the silkworm as a model organism to study the impact of high PPC on female reproduction. However, it is important to note that the characteristics of silkworm differ significantly from those of humans. Therefore, the next step should validate the mechanism discovered in this article on other model animals, such as flies and mice. This cross-species validation will provide further insights and strengthen the generalizability of our findings.

### STAR★METHODS

Detailed methods are provided in the online version of this paper and include the following:

- KEY RESOURCES TABLE
- RESOURCE AVAILABILITY
  - Lead contact
  - Materials availability
  - Data and code availability
- EXPERIMENTAL MODEL AND STUDY PARTICIPANT DETAILS
  - Preparation of animals
  - Reproduction testing
  - Ovarian transcriptomic sequencing analysis
  - qRT-PCR
  - Western blotting
  - Biochemical testing
  - Drugs injection
- QUANTIFICATION AND STATISTICAL ANALYSIS

### SUPPLEMENTAL INFORMATION

Supplemental information can be found online at <https://doi.org/10.1016/j.isci.2023.107860>.

### ACKNOWLEDGMENTS

This study was supported by the National Natural Science Foundation of China (No. 31972625), China Postdoctoral Science Foundation (No. 2020M681718), Priority Academic Program Development of Jiangsu Higher Education Institutions (PAPD) of Jiangsu Higher Education Institutions, and the Postgraduate Research & Practice Innovation Program of Jiangsu Province (No. KYCX23\_3259).

### AUTHOR CONTRIBUTIONS

S.Q.X., G.H.J., and G.W. conceived this project. G.H.J., G.W., C.L., Y.F.W., J.F.Q., R.J.P., and Y.H.S. performed the research. G.H.J., G.W., and S.Q.X. analyzed the data and wrote the paper. All authors participated in the revision of this paper.

### DECLARATION OF INTERESTS

The authors declare no competing interests.

### INCLUSION AND DIVERSITY

We support inclusive, diverse, and equitable conduct of research.

Received: May 16, 2023

Revised: August 11, 2023

Accepted: September 6, 2023

Published: September 9, 2023

### REFERENCES

1. Kitazawa, A., Koda, R., Yoshino, A., Ueda, Y., and Takeda, T. (2018). An IgA1-lambda-type monoclonal immunoglobulin deposition disease associated with membranous features in a patient with IgG4-related kidney disease: a case report. *BMC Nephrol.* 19, 330. <https://doi.org/10.1186/s12882-018-1133-9>.
2. Schmidt, F.W., and Wildhirt, E. (1957). Hyperproteinämie und myelomähnliche Serumeiweißbilder bei der Lebercirrhose. *Klin. Wochenschr.* 35, 1139–1144. <https://doi.org/10.1007/BF01489421>.
3. Eberhardt, C., Malbon, A., Riond, B., and Schoster, A. (2018).  $\kappa$  Light-chain monoclonal gammopathy and cast nephropathy in a horse with multiple myeloma. *J. Am. Vet. Med. Assoc.* 253, 1177–1183. <https://doi.org/10.2460/javma.253.9.1177>.
4. Hussain, A., Almenfi, H.F., Almehdewi, A.M., Hamza, M.S., Bhat, M.S., and Vijayashankar, N.P. (2019). Laboratory features of newly diagnosed multiple myeloma patients. *Cureus* 11, e4716. <https://doi.org/10.7759/cureus.4716>.
5. Gama, M.E.A., Costa, J.M.L., Gomes, C.M.C., and Corbett, C.E.P. (2004). Subclinical form of the American visceral

- leishmaniasis. *Mem. Inst. Oswaldo Cruz* 99, 889–893. <https://doi.org/10.1590/s0074-02762004000800018>.
6. Urbani, L., Tirolo, A., Salvatore, D., Tumbarello, M., Segatore, S., Battilani, M., Balboni, A., and Dondi, F. (2020). Serological, molecular and clinicopathological findings associated with *Leishmania infantum* infection in cats in Northern Italy. *J. Feline Med. Surg.* 22, 935–943. <https://doi.org/10.1177/1098612X19895067>.
  7. Niitsu, N., Kohri, M., Hayama, M., Nakamine, H., Nakamura, N., Bessho, M., and Higashihara, M. (2005). Primary pulmonary plasmacytoma involving bilateral lungs and marked hypergammaglobulinemia: differentiation from extranodal marginal zone B-cell lymphoma of mucosa-associated lymphoid tissue. *Leuk. Res.* 29, 1361–1364. <https://doi.org/10.1016/j.leukres.2005.04.009>.
  8. Wang, G., Wang, Y.F., Li, J.L., Peng, R.J., Liang, X.Y., Chen, X.D., Jiang, G.H., Shi, J.F., Sima, Y.H., and Xu, S.Q. (2022). Mechanism of hyperproteinemia-induced blood cell homeostasis imbalance in an animal model. *Zool. Res.* 43, 301–318. <https://doi.org/10.2472/zj.issn.2095-8137.2021.397>.
  9. Manning, R.D. (1987). Renal hemodynamic, fluid volume, and arterial pressure changes during hyperproteinemia. *Am. J. Physiol.* 252, F403–F411. <https://doi.org/10.1152/ajprenal.1987.252.3.F403>.
  10. Perlzweig, W.A., Delrue, G., and Geschickter, C. (1928). Hyperproteinemia associated with multiple myelomas. *J. Am. Med. Assoc.* 90, 755–757. <https://doi.org/10.1001/jama.1928.02690370023011>.
  11. Abuzaid, A.A., Aldahan, M.A., Helal, M.A.A., Assiri, A.M., and Alzahran, M.H. (2020). Visceral leishmaniasis in Saudi Arabia: From hundreds of cases to zero. *Acta Trop.* 212, 105707. <https://doi.org/10.1016/j.actatropica.2020.105707>.
  12. Becerra, J.E., Khoury, M.J., Cordero, J.F., and Erickson, J.D. (1990). Diabetes mellitus during pregnancy and the risks for specific birth defects: a population-based case-control study. *Pediatrics* 85, 1–9.
  13. Gesink Law, D.C., Maclehorse, R.F., and Longnecker, M.P. (2007). Obesity and time to pregnancy. *Hum. Reprod.* 22, 414–420. <https://doi.org/10.1093/humrep/del400>.
  14. Lüscher, B.P., Schoeberlein, A., Surbek, D.V., and Baumann, M.U. (2022). Hyperuricemia during pregnancy leads to a preeclampsia-like phenotype in mice. *Cells* 11, 3703. <https://doi.org/10.3390/cells11223703>.
  15. Ratchford, A.M., Chang, A.S., Chi, M.M.Y., Sheridan, R., and Moley, K.H. (2007). Maternal diabetes adversely affects AMP-activated protein kinase activity and cellular metabolism in murine oocytes. *Am. J. Physiol. Endocrinol. Metab.* 293, E1198–E1206. <https://doi.org/10.1152/ajpendo.00097.2007>.
  16. Wang, Q., Chi, M.M., Schedl, T., and Moley, K.H. (2012). An intercellular pathway for glucose transport into mouse oocytes. *Am. J. Physiol. Endocrinol. Metab.* 302, E1511–E1518. <https://doi.org/10.1152/ajpendo.00016.2012>.
  17. Moraes-Souza, R.Q., Sinzato, Y.K., Antunes, B.T., Umeoka, E.H.L., Oliveira, J.A.C., Garcia-Cairasco, N., Karki, B., Volpato, G.T., and Damasceno, D.C. (2020). Evaluation of maternal reproductive outcomes and biochemical analysis from Wistar Audiogenic Rats (WAR) and repercussions in their offspring. *Reprod. Sci.* 27, 2223–2231. <https://doi.org/10.1007/s43032-020-00236-0>.
  18. Schäfer, M., Tran, T.H., Paarmann, S., and Kramer, G. (1990). Beziehungen zwischen stoffwechselstatus und ergebnis der embryogewinnung bei hochleistungskühen [Relationship between metabolic status and results of embryo collection in high-producing cows]. *Arch. Exp. Veterinaarmed.* 44, 157–162.
  19. Chen, X.D., Wang, Y.F., Wang, Y.L., Li, Q.Y., Ma, H.Y., Wang, L., Sima, Y.H., and Xu, S.Q. (2018). Induced hyperproteinemia and its effects on the remodeling of fat bodies in silkworm, *Bombyx mori*. *Front. Physiol.* 9, 302–309. <https://doi.org/10.3389/fphys.2018.00302>.
  20. Wang, Y.F., Wang, G., Li, J.L., Qu, Y.X., Liang, X.Y., Chen, X.D., Sima, Y.H., and Xu, S.Q. (2021). Influence of hyperproteinemia on insect innate immune function of the circulatory system in *Bombyx mori*. *Biology* 10, 112. <https://doi.org/10.3390/biology10020112>.
  21. Chen, X., Wang, Y., Wang, Y., Li, Q., Liang, X., Wang, G., Li, J., Peng, R., Sima, Y., and Xu, S. (2022). Ectopic expression of sericin enables efficient production of ancient silk with structural changes in silkworm. *Nat. Commun.* 13, 6295. <https://doi.org/10.1038/s41467-022-34128-5>.
  22. Xia, Q., Li, S., and Feng, Q. (2014). Advances in silkworm studies accelerated by the genome sequencing of *Bombyx mori*. *Annu. Rev. Entomol.* 59, 513–536. <https://doi.org/10.1146/annurev-ento-011613-161940>.
  23. Wang, H., Wang, L., Wang, Y., Tao, H., Yin, W., SiMa, Y., Wang, Y., and Xu, S. (2015). High yield exogenous protein HPL production in the *Bombyx mori* silk gland provides novel insight into recombinant expression systems. *Sci. Rep.* 5, 13839. <https://doi.org/10.1038/srep13839>.
  24. Cui, W.Z., Qiu, J.F., Dai, T.M., Chen, Z., Li, J.L., Liu, K., Wang, Y.J., Sima, Y.H., and Xu, S.Q. (2021). Circadian clock gene period contributes to diapause via GABAergic-diapause hormone pathway in *Bombyx mori*. *Biology* 10, 842. <https://doi.org/10.3390/biology10090842>.
  25. Miller, G.L. (1959). Use of dinitrosalicylic acid reagent for determination of reducing sugar. *Anal. Chem.* 31, 426–428. <https://doi.org/10.1021/ac60147a030>.
  26. Wang, L., Kiuchi, T., Fujii, T., Daimon, T., Li, M., Banno, Y., Kikuta, S., Kikawada, T., Katsuma, S., and Shimada, T. (2013). Mutation of a novel ABC transporter gene is responsible for the failure to incorporate uric acid in the epidermis of ok mutants of the silkworm, *Bombyx mori*. *Insect Biochem. Mol. Biol.* 43, 562–571. <https://doi.org/10.1016/j.ibmb.2013.03.011>.
  27. Jiang, G., Song, J., Hu, H., Tong, X., and Dai, F. (2020). Evaluation of the silkworm lemon mutant as an invertebrate animal model for human septiprotein reductase deficiency. *R. Soc. Open Sci.* 7, 191888. <https://doi.org/10.1098/rsos.191888>.
  28. Matsumoto, Y., Ishii, M., Hayashi, Y., Miyazaki, S., Sugita, T., Sumiya, E., and Sekimizu, K. (2015). Diabetic silkworms for evaluation of therapeutically effective drugs against type II diabetes. *Sci. Rep.* 5, 10722. <https://doi.org/10.1038/srep10722>.
  29. Matsumoto, Y., and Sekimizu, K. (2016). Evaluation of anti-diabetic drugs by using silkworm, *Bombyx mori*. *Drug Discov. Ther.* 10, 19–23. <https://doi.org/10.5582/ddt.2016.01017>.
  30. Yang, C., Lin, Y., Liu, H., Shen, G., Luo, J., Zhang, H., Peng, Z., Chen, E., Xing, R., Han, C., and Xia, Q. (2014). The Broad Complex isoform 2 (BrC-Z2) transcriptional factor plays a critical role in vitellogenin transcription in the silkworm *Bombyx mori*. *Biochim. Biophys. Acta* 1840, 2674–2684. <https://doi.org/10.1016/j.bbagen.2014.05.013>.
  31. Kamei, Y., Hasegawa, Y., Niimi, T., Yamashita, O., and Yaginuma, T. (2011). Trehalase-2 protein contributes to trehalase activity enhanced by diapause hormone in developing ovaries of the silkworm, *Bombyx mori*. *J. Insect Physiol.* 57, 608–613. <https://doi.org/10.1016/j.jinsphys.2010.10.001>.
  32. Chen, E., Chen, Z., Li, S., Xing, D., Guo, H., Liu, J., Ji, X., Lin, Y., Liu, S., and Xia, Q. (2020). bmo-miR-2739 and the novel microRNA miR-167 coordinately regulate the expression of the vitellogenin receptor in *Bombyx mori* oogenesis. *Development* 147, dev183723. <https://doi.org/10.1242/dev.183723>.
  33. Zhu, Z., Tong, C., Qiu, B., Yang, H., Xu, J., Zheng, S., Song, Q., Feng, Q., and Deng, H. (2021). 20E-mediated regulation of BmKr-h1 by BmKRP promotes oocyte maturation. *BMC Biol.* 19, 39. <https://doi.org/10.1186/s12915-021-00952-2>.
  34. Shen, G., Wu, J., Han, C., Liu, H., Xu, Y., Zhang, H., Lin, Y., and Xia, Q. (2018). Oestrogen-related receptor reduces vitellogenin expression by crosstalk with the ecdysone receptor pathway in female silkworm, *Bombyx mori*. *Insect Mol. Biol.* 27, 454–463. <https://doi.org/10.1111/imb.12385>.
  35. Wang, Y.F., Chen, X.D., Wang, G., Li, Q.Y., Liang, X.Y., Sima, Y.H., and Xu, S.Q. (2019). Influence of hyperproteinemia on reproductive development in an invertebrate model. *Int. J. Biol. Sci.* 15, 2170–2181. <https://doi.org/10.7150/ijbs.33310>.
  36. Barbieri, R.L. (2008). Update in female reproduction: a life-cycle approach. *J. Clin. Endocrinol. Metab.* 93, 2439–2446. <https://doi.org/10.1210/jc.2008-0752>.
  37. Yang, J., Cummings, E.A., O'connell, C., and Jangaard, K. (2006). Fetal and neonatal outcomes of diabetic pregnancies. *Obstet. Gynecol.* 108, 644–650. <https://doi.org/10.1097/01.AOG.0000231688.08263.47>.
  38. Moley, K.H., Chi, M.M., and Mueckler, M.M. (1998). Maternal hyperglycemia alters glucose transport and utilization in mouse preimplantation embryos. *Am. J. Physiol.* 275, E38–E47. <https://doi.org/10.1152/ajpendo.1998.275.1.E38>.

## STAR★METHODS

### KEY RESOURCES TABLE

REAGENT or RESOURCE	SOURCE	IDENTIFIER
<b>Antibodies</b>		
Rabbit monoclonal anti-p-AKT (S473)	Cell Signaling Technology	Cat# 4060; RRID: AB_2315049
Rabbit monoclonal anti-AKT	Cell Signaling Technology	Cat# 4691; RRID: AB_915783
Mouse monoclonal anti- $\beta$ -actin	Santa Cruz Biotechnology	Cat# sc-47778; RRID: AB_626632
Mouse monoclonal anti- $\beta$ -tubulin	Abmart	Cat# M20005; RRID: AB_2920648
HRP-labeled goat anti-rabbit secondary antibody	MultiSciences	Cat# GAR007; RRID: AB_2827833
HRP-labeled goat anti-mouse secondary antibody	MultiSciences	Cat# GAM007; RRID: AB_2927718
Rabbit monoclonal anti-HPL	Abmart	N/A
<b>Chemicals, peptides, and recombinant proteins</b>		
TRIzol™	Invitrogen	Cat# 15596018
RIPA Lysis Buffer	Beyotime	Cat# P0013B
Potassium sodium tartrate	HUSHI	Cat# 10017818; CAS: 6381-59-5
3,5-Dinitrosalicylic acid	HUSHI	Cat# 30073424; CAS: 609-99-4
Sodium hydroxide	HUSHI	Cat# 10019762; CAS: 1310-73-2
Phenol	HUSHI	Cat# 40040761; CAS: 108-95-2
Bovine insulin	Yuanye	Cat# S12033; CAS: 11070-73-8
Trehalose	Macklin	Cat# D807342; CAS: 99-20-7
LY294002	Beyotime	Cat# S1737; CAS: 154447-36-6
<b>Critical commercial assays</b>		
PrimeScript™ RT reagent Kit (Perfect Real Time)	TaKaRa	Cat# RR037B
Glycogen assay kit	COMIN	Cat# TY-1-Y
BCA protein assay kit	Beyotime	Cat# P0012
<b>Deposited data</b>		
Raw RNA-seq data	This paper	GEO: GSE242203
<b>Experimental models: Organisms/strains</b>		
Female Silkworm ( <i>Bombyx mori</i> )	School of Biology and Basic Medical Sciences, Suzhou Medical College, Soochow University	N/A
<b>Oligonucleotides</b>		
See Table S1 for the Primers used in qRT-PCR	This paper	N/A
<b>Software and algorithms</b>		
GraphPad Prism 8	La Jolla, CA, USA	<a href="https://www.graphpad.com/">https://www.graphpad.com/</a>
ImageJ	National Institutes of Health	<a href="https://imagej.nih.gov/ij/">https://imagej.nih.gov/ij/</a>

## RESOURCE AVAILABILITY

### Lead contact

Further information and requests for resources, reagents and original data should be directed to and will be fulfilled by the lead contact, Shi-Qing Xu. ([szsqxu@suda.edu.cn](mailto:szsqxu@suda.edu.cn)).

### Materials availability

This study did not generate new unique reagents.

### Data and code availability

- All data reported in this paper will be shared by the [lead contact](#) upon request.
- Ovarian RNA-seq data have been deposited at GEO and are publicly available on Sep 06, 2023. Accession numbers are listed in the [key resources table](#).
- This paper does not report original code.
- Any additional information required to analyze the data reported in this paper is available from the [lead contact](#) upon request.

## EXPERIMENTAL MODEL AND STUDY PARTICIPANT DETAILS

### Preparation of animals

The high PPC model animal is a transgenic *Bombyx mori* called TBH (*Hpl/Hpl*) which was inserted a 3057 bp full-length coding sequence of fibroin heavy chain protein-like gene (*Hpl*) into its genome, and the *Hpl* is expressed specifically in the posterior silk gland of TBH larvae.<sup>23</sup> Due to the difficulty associated with spinning silk in mature TBH larvae (wandering stage, W), a large amount of silk protein remaining in the silk gland cavity is released into the hemolymph during the degeneration of the silk gland, resulting in a continuous increase of PPC. The female N4 strain was used as wild-type silkworm (WT). A mAM, with a similar PPC level as TBH, was generated by blocking the spinnerets of female WT silkworms using paraffin wax (55°C–60°C) after spinning for 24 h in the wandering stage.<sup>8</sup> Silkworm larvae were reared with fresh mulberry leaves, and the living environment for the whole generation was maintained at 25°C, 75% relative humidity, and with a 12 h light/12 h dark photoperiod.

At the scheduled time, hemolymph samples were collected by piercing the dorsal vessels of the female silkworm. Subsequently, the female silkworms were dissected on an ice bath with a scalpel to separate the intact silk glands and ovaries, as well as fat bodies from the abdomen and back. The tissues samples were then washed in pre-cooled physiological saline and transferred to 1.5 mL centrifuge tubes for further experiments. Each tissue sample comprised an equal mixture of multiple silkworm individuals.

### Reproduction testing

The weight of three female silkworms and their complete ovaries were measured to calculate the gonadosomatic index (GSI, GSI = weight of ovary/weight of silkworm). This measurement was performed on three groups at different timepoints, including the wandering and pupal stages (n = 3). The morphology of the ovaries was captured using a camera (EOS 70D, Canon, Tokyo, Japan) to observe the developmental process of the ovaries.

The number of eggs laid within 24 h by each female moth and the count of remaining eggs in their ovary tubes was recorded (n = 15). The combined count of these eggs represented the total number of eggs produced by an individual moth. The laid eggs (n = 6) were reared at 25°C with 75% relative humidity for 10 days to calculate the number of eggs in the body pigmentation stage (EP) and the number of eggs in the body no-pigmentation stage (no-EP). The EP rate = EP/(EP + no-EP).

### Ovarian transcriptomic sequencing analysis

Ovary samples for RNA-sequencing (RNA-seq) were obtained by dissecting five female pupae at the P2 and P4 stages (n = 3). The construction and sequencing of the transcriptional library was carried out by Shanghai Majorbio Bio-Pharm Technology Co., Ltd. (Shanghai, China) using the Illumina Novaseq 6000 platform. Genome and gene model annotation referred to the silkworm database ([http://metazoa.ensembl.org/Bombyx\\_mori/Info/Index](http://metazoa.ensembl.org/Bombyx_mori/Info/Index)). The expression levels of genes and new transcripts were assessed by Transcripts Per Kilobase per Million mapped reads (TPM). DESeq2 software was used to determine difference in gene expression between groups and the screening thresholds were  $|\log_2FC| \geq 1$  and p-adjust < 0.05.

### qRT-PCR

Total RNA was extracted from ovaries or silk gland samples (n = 3) using TRIzol reagent (15596018, Invitrogen, USA), and cDNA was obtained using a PrimeScript RT reagent Kit (Perfect Real Time) (RR037B, TaKaRa, Dalian, China). qRT-PCR was carried out by an ABI StepOnePlus real-time quantitative fluorescent PCR system (Ambion, Foster City, CA, USA). *sw22934* and *Rp49* were used as reference genes. The primer sequences were designed using Primer Premier 5 (Table S1).

### Western blotting

Western blotting was conducted following the previously reported method.<sup>8</sup> Total protein from the silk gland or fat body samples (n = 3) was extracted with RIPA Lysis Buffer (P0013B, Beyotime, Shanghai, China), and 10% sodium dodecyl sulfate-polyacrylamide gel electrophoresis was performed. The primary antibodies included purified anti-HPL antibody (1:1000), anti-p-AKT antibody (S473) (1:2000; 4060, Cell Signaling Technology, USA), and anti-AKT antibody (1:1000; 4691, Cell Signaling Technology, USA), all of which are rabbit antibodies. The internal reference antibodies were anti-β-actin antibody (1:1000; sc-47778, Santa Cruz Biotechnology, USA) and anti-β-tubulin antibody (1:5000; M20005, Abmart, China), all of which are mouse antibodies. The second antibodies were HRP-labeled goat anti-rabbit or goat anti-mouse IgG (1:5000; GAR007/GAM007, MultiSciences, China). The HPL protein antibody was prepared by Abmart Shanghai Co., Ltd. (Shanghai, China), and the polypeptide sequence NENNHNDNTR-C was used as the antigen to generate immunity in New Zealand white rabbits.

### Biochemical testing

Hemolymph samples ( $n = 3$ ) were used for the determination of PPC, trehalose and glucose content. Samples ( $n = 3$ ) of ovaries, fat bodies and laid eggs were used for glycogen determination. The absorbance was detected by an Enzyme-labeled instrument (Eon, BioTek, USA).

The hemolymph samples were centrifuged at 1000  $g$  and 4°C for 10 min to collect the supernatants for further testing. PPC was detected with a BCA protein assay kit (P0012, Beyotime, Shanghai, China) in accordance with the manufacturer's instructions, and the absorbance at 562 nm was measured. The PPC ratio was calculated by normalizing the PPC of WT and then dividing the PPC of TBH silkworms by that of WT.

The trehalose content was determined by the anthrone method.<sup>24</sup> 10  $\mu$ L of hemolymph samples were mixed with 150  $\mu$ L of 80% ethanol, heated for 20 min at 78°C in a metal bath (CHB-100, Bioer Technology, Zhejiang, China), and then centrifuged at 4000  $g$  for 10 min to collect the supernatants. The precipitate was mixed with 50  $\mu$ L of 80% ethanol and then re-treated with the same procedure. All supernatants were dried in a metal bath at 70°C for ~2 h. The absorbance at 620 nm was measured after the anthrone reaction.

Glucose content was determined by the Ghose method.<sup>25</sup> Hemolymph samples were centrifuged at 900  $g$  and 4°C for 5 min to collect the supernatants. Then, 10  $\mu$ L of supernatant and 200  $\mu$ L of DNS reagent (18.2 g of potassium sodium tartrate, 0.63 g of 3,5-dinitrosalicylic acid, 2.1 g of sodium hydroxide, 0.5 g of phenol, with pure water to 100 mL) were mixed and heated at 100°C for 5 min. The absorbance was measured at 540 nm after cooling.

The glycogen content in samples from the fat bodies, ovaries and laid eggs was detected by a glycogen assay kit (TY-1-Y, Comin, Suzhou, China) according to the manufacturer's instructions. The absorption value at 620 nm was then measured.

### Drugs injection

One-day-old female pupae (P1) were injected with 10  $\mu$ L of bovine insulin (CAS No. 11070-73-8, Yuanye, Shanghai, China), trehalose (CAS No. 99-20-7, Macklin, Shanghai, China) and 0.1 nmol/mL LY294002 (CAS No. 154447-36-6, Beyotime, Shanghai, China). Injections were performed into the VIII dorsal intersegmental membrane with a glass capillary tube to investigate blood sugar level and the adult reproductive index. The concentration of bovine insulin was 2, 6, and 10  $\mu$ g/ $\mu$ L, and that of trehalose was 0.05, 0.1, and 0.5 mg/ $\mu$ L. The control group was injected with the same volume of saline solution.

### QUANTIFICATION AND STATISTICAL ANALYSIS

GraphPad Prism 8 software (La Jolla, CA, USA) was used to analyze statistical data and the results are shown as mean  $\pm$  standard deviation (SD). Data were analyzed by the Student's  $t$  test or variance (ANOVA). A  $p$ -value  $< 0.05$  was considered significant, which is indicated as ns,  $p > 0.05$ ; \*,  $p < 0.05$ ; \*\*,  $p < 0.01$ ; \*\*\*,  $p < 0.001$ .